PHYSICAL REVIEW A **94**, 013416 (2016)

Photon-energy dependence of single-photon simultaneous core ionization and core excitation in CO_2

S. Carniato,[1,*] P. Selles,[1] P. Lablanquie,[1] J. Palaudoux,[1] L. Andric,[1,2] M. Nakano,[3,4] Y. Hikosaka,[5] K. Ito,[3] T. Marchenko,[1]
O. Travnikova,[1] G. Goldsztejn,[1] L. Journel,[1] R. Guillemin,[1] D. Céolin,[6] M. Simon,[1,6] M. N. Piancastelli,[1,7] and F. Penent[1]
[1]*Sorbonne Universités, UPMC Univ Paris 06, CNRS, LCP-MR (UMR 7614), 11 rue Pierre et Marie Curie, 75231 Paris Cedex 05, France*
[2]*Université Paris-Est, 5 boulevard Descartes, F-77454 Marne-la Vallée Cedex 2, France*
[3]*Photon Factory, Institute of Materials Structure Science, Oho, Tsukuba 305-0801, Japan*
[4]*Department of Chemistry, Tokyo Institute of Technology, O-okayama, Tokyo 152-8551, Japan*
[5]*Graduate School of Medicine and Pharmaceutical Sciences, University of Toyama, Toyama 930-0194, Japan*
[6]*Synchrotron SOLEIL, l'Orme des Merisiers, Saint-Aubin, Boîte Postale 48, 91192 Gif-sur-Yvette Cedex, France*
[7]*Department of Physics and Astronomy, Uppsala University, P.O. Box 516, 75120, Uppsala, Sweden*

(Received 18 March 2016; published 20 July 2016)

We have studied the $K^{-2}V$ process corresponding to simultaneous K-shell ionization and K-shell excitation in the CO_2 molecule. We define these $K^{-2}V$ states as super shake-up, at variance with the "conventional" $K^{-1}v^{-1}V$ shake-up states. While the nature and evolution with photon energy of the conventional shake-up satellites has been the object of many studies, no such data on a large photon-energy range were previously reported on super shake-up. The CO_2 molecule is a textbook example because it exhibits two well-isolated $K^{-2}V$ resonances (with V being $2\pi_u^*$ and $5\sigma_g^*$) with different symmetries resulting from shake-up processes of different origin populated in comparable proportions. The variation of the excitation cross section of these two resonances with photon energy is reported, using two different experimental approaches, which sheds light on the excitation mechanisms. Furthermore, double-core-hole spectroscopy is shown to be able to integrate and even expand information provided by conventional single-core-hole X-ray Photoelectron Spectroscopy (XPS) and Near-Edge X-ray Absorption Fine Structure (NEXAFS) techniques, revealing, for instance, g-g dipole forbidden transitions which are only excited in NEXAFS spectra through vibronic coupling.

DOI: 10.1103/PhysRevA.94.013416

I. INTRODUCTION

Double-core-hole (DCH) spectroscopy has aroused strong experimental and theoretical interest since 2009 because it exhibits a stronger sensitivity to chemical environment than conventional single-core-hole spectroscopy and has benefited from the advent of intense X-ray Free Electron Laser (X-FEL) sources allowing two-photon processes in the x-ray domain [1]. Independently, due to improvements in coincident electron spectroscopy, it became also possible to perform high-resolution single-photon DCH spectroscopy on synchrotron centers. Single-site (K^{-2}) and two-site ($K^{-1}K^{-1}$) DCH states have been studied by single-photon absorption although they represent only a tiny ($\sim10^{-3}$–10^{-5}) fraction of the K^{-1} dominant ionization process [2,3]. Among those DCH states, $K^{-2}V$ states corresponding to simultaneous K-shell ionization and K-shell excitation have been observed recently [4–7] and present a specific interest for spectroscopy because two excitation pathways, with comparable intensities, are possible. The corresponding photoelectron spectra were very well reproduced by a theoretical model [6] taking those two pathways into account. Following the designation introduced by Martin and Shirley [8] for "conventional" satellite states ($K^{-1}v^{-1}V$), also $K^{-2}V$ satellites can be categorized as "direct" or "conjugate." The direct shake-up is described by dipolar K-shell ionization accompanied by monopolar excitation (shake-up) of the remaining K-shell electron, while the conjugate shake-up is described by dipolar excitation of a K-shell electron to a vacant V orbital accompanied by monopolar ionization (shake-off) of the remaining K-shell electron.

Excitation of $K^{-2}V$ states can hence be considered as a "super" shake-up process where the "shaken" electron is the remaining K-shell electron. For conventional satellite states ($K^{-1}v^{-1}V$) the direct shake-up process is generally much stronger than the conjugate channel that is more visible close to threshold [9]. One of our goals is to study the evolution, with photon energy, of conjugate versus direct contributions for the new $K^{-2}V$ shake-up process. Our previous experimental observation showed similar direct and conjugate cross sections confirmed on an absolute scale by our theoretical model [6] though only a moderate photon-energy dependence of the two pathways could be observed in the case of N_2 [7] in a limited photon-energy range ($h\nu = 950$–$1150\,\text{eV}$).

In the present paper, we have studied the $K^{-2}V$ process in the centrosymmetric CO_2 molecule. Its peculiarity is that the first two $K^{-2}V$ resonances, below the carbon K^{-2} edge, are well isolated from each other and from higher-lying resonances and are clearly identified as conjugate and direct shake-up pathways. We have hence a very clean situation. We have observed this process at very different excess energies above the K^{-2} threshold ($\sim$100 and 1650 eV) to study the evolution of direct and conjugate shake-up channels on a broad energy range in order to understand the very nature of their excitation mechanisms. These measurements provide also accurate relative cross sections with respect to single-K-shell ionization that can be converted in absolute cross sections directly comparable with theoretical values. Furthermore, we show that such spectroscopy can provide information not available by conventional single-hole spectroscopy, by allowing the investigation of resonant processes not visible in absorption spectroscopy due to dipole selection rules.

---

[*] stephane.carniato@upmc.fr

II. EXPERIMENTS

Two different experiments have been performed. The first one was described in our previous works [5] and relies on a magnetic bottle time-of-flight spectrometer. We detect one photoelectron in coincidence with two Auger electrons to identify the $K^{-2}V$ process specifically:

$$\begin{aligned} h\nu + \mathrm{CO_2} &\rightarrow \{[\mathrm{C}(K^{-2})\mathrm{O_2}]V\}^{+} + e^{-}_{\mathrm{ph}} \\ &\rightarrow \{[\mathrm{C}(K^{-1})\mathrm{O_2}]v^{-2}V\}^{2+} + e^{-}_{A1} \\ &\rightarrow \{\mathrm{CO_2}v^{-4}V\}^{3+} + e^{-}_{A2}. \end{aligned}$$

The experiments were performed on the BL16 beamline in Photon Factory (PF) in Tsukuba (Japan). The experimental setup, the photon-energy calibration, the time-of-flight to energy conversion, and the detection efficiency determination experimental procedures, were described in detail in previous references [2,3,5,10,11]. The photon energy was chosen at 760 eV to keep a good enough (∼1.7 eV) energy resolution for the $K^{-2}V$ photoelectrons and favorable conditions to observe also the K^{-2} process.

The second experiment relies on the detection of the specific photoelectron associated to the $K^{-2}V$ process. As long as the energy of those photoelectrons is well separated from dominant photoelectron or Auger lines, it is possible to observe the corresponding specific photoelectron lines with a conventional high-performance electron spectrometer [12,13]. The hemispherical deflection analyzer (HDA 180°) (Scienta EW4000 HAXPES) installed on the GALAXIES beamline in the SOLEIL synchrotron radiation facility (Saint-Aubin, France) fulfills these goals [14]. The beamline and the spectrometer are described in detail elsewhere [15].

III. EXPERIMENTAL RESULTS AND THEORETICAL INTERPRETATION

A. Results at $h\nu = 760$ eV

The $K^{-2}V$ photoelectron spectra obtained at 760 eV are presented in Fig. 1 with the K^{-2} signal (deduced from four electron coincidences [2]), as a function of the binding energy. The interpretation of the spectra at $h\nu = 760$ eV is supported by the theoretical model. The dominant configuration of the $\mathrm{CO_2}$ molecule in its ground electronic state is $[1\sigma_g^2\,1\sigma_u^2\,2\sigma_g^2\,3\sigma_g^2\,2\sigma_u^2\,4\sigma_g^2\,3\sigma_u^2\,1\pi_u^4\,1\pi_g^4]$ where the $1\sigma_g$ and $1\sigma_u$ orbitals are linear combinations of the two O 1s orbitals and the $2\sigma_g$ corresponds to the C 1s orbital. The first four unoccupied orbitals of interest are the $2\pi_u^*$ [lowest unoccupied molecular orbital (LUMO)], $5\sigma_g^*$,$3s\sigma_g$, and $4\sigma_u^*$ orbitals.

The positions of the K^{-2} threshold and of the $K^{-2}V$ resonances have been obtained at a DFT/B3LYP level of theory. The K^{-2} threshold is found at 665.05 eV, the first resonance, A, at 643.91 eV, and the second one, B, at 649.68 eV, in good agreement with the experimental values of 666.0 ± 1 eV, 645.6 ± 1 eV, and 650 ± 1 eV, respectively. In Fig. 1, an overall shift has been applied to the theoretical spectrum so that peak A corresponds to the experimental value. The theoretical spectrum takes into account a lifetime broadening

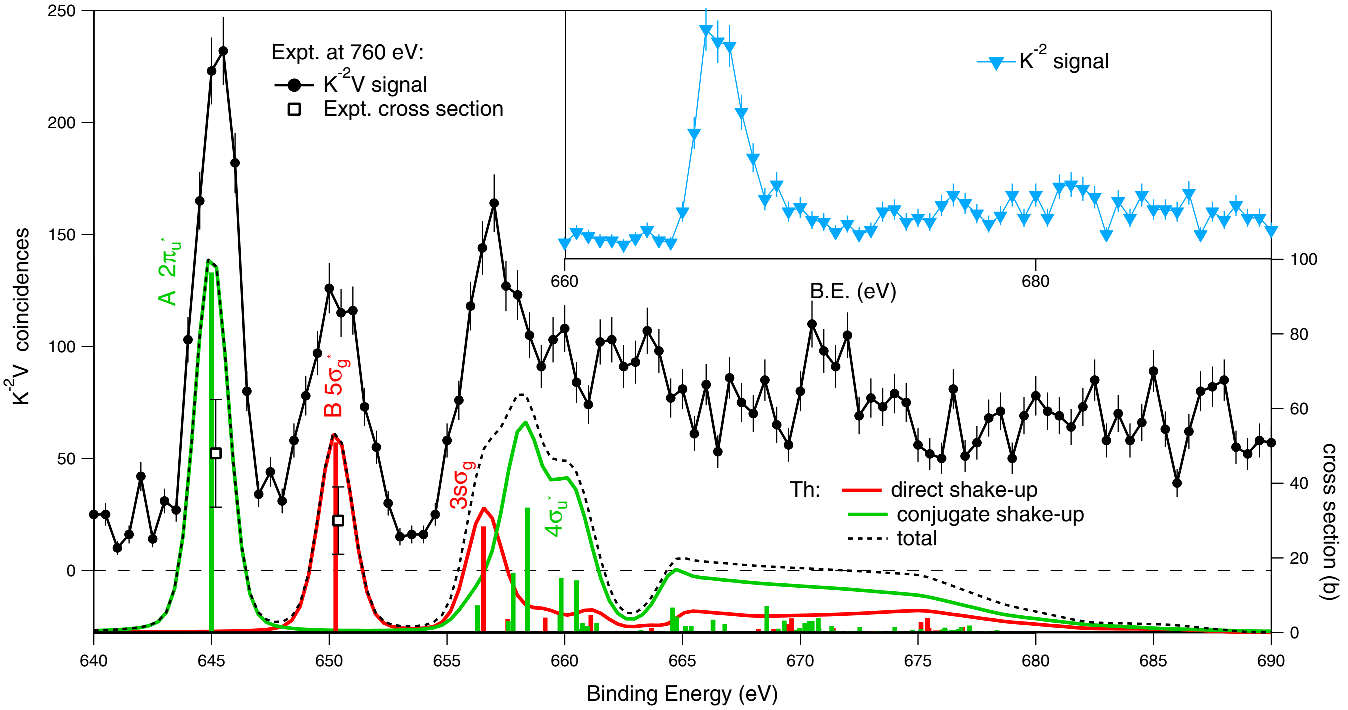

FIG. 1. At $h\nu = 760$ eV, experimental $K^{-2}V$ and K^{-2} spectra at the C K^{-2} edge in $\mathrm{CO_2}$ obtained by filtering three- and four-electron coincident events. The photoelectron(s) are coincident with hypersatellite Auger (260–320 eV) and second Auger (225–260 eV) electrons. Electrons below 5 eV have been rejected from the K^{-2} signal to reduce the noise. The $K^{-2}V$ theoretical spectra show direct (red line and bars) and conjugate (green line and bars) contributions. Vertical bars give the integrated theoretical cross sections for each peak. Experimental absolute cross sections (□) include an additional 30% contribution from second Auger electrons (190–225 eV) falling in the same energy range than O(1s) photoelectrons.

of 3 × 99 meV (3 times those of the CO_2 K^{-1} states, [16]) and an experimental resolution of 1.65 eV. The integrated cross sections for all peaks are given by vertical bars in Fig. 1.

The electronic structure of each peak is revealed with a post–Hartree-Fock configuration Interaction model [6]. The first two peaks A and B are of different natures. The first resonance A results from pure conjugate shake-up. It is almost exclusively built on the $K^{-2}(2\pi_u^*)$ configuration. This resonance is the strongest one, as it is in Near-Edge X-ray Absorption Fine Structure (NEXAFS) carbon K-edge spectra where the $1s \to 2\pi_u^*$ line is the dominant one at 290.77 eV [17]. The second resonance B results from pure direct shake-up. It is almost entirely built on the $K^{-2}(5\sigma_g^*)$ configuration. This resonance corresponds hence to the ionization of a C $1s$ electron together with a $1s \to 5\sigma_g^*$ shake-up. In the NEXAFS carbon K-edge spectra, the $1s \to 5\sigma_g^*$ line does not appear due to dipolar selection rules, which illustrates one of the advantages of $K^{-2}V$ spectroscopy. In the region around 660 eV many Rydberg as well as multiple core-valence excitation resonances are found. Among them excitation of the $3s\sigma_g$ Rydberg orbital is largely responsible for the left side structure of the peak at 656.5 eV. The corresponding $1s \to 3s\sigma_g$ line is also dipole forbidden and only appears in NEXAFS spectra due to vibronic couplings [18]. The central maximum around 657 eV is assigned to the $4\sigma_u^*$ resonance, which is observed as a shape resonance σ_u^* 14 eV above the K^{-1} threshold in NEXAFS spectra [19,20]. The shift below the K^{-2} ionization threshold of σ^* resonances usually observed above ionization threshold in NEXAFS spectra has already been identified as a characteristic of $K^{-2}V$ spectroscopy in N_2 and H_2O molecules [6,7]. This finding sheds further light on the nature of such resonances, which has been highly controversial in the literature (see, e.g., [21]). In particular, their analogy with virtual molecular orbitals rather than scattering by the nuclei is confirmed. The valence character of $2\pi_u^*$, $5\sigma_g^*$, and $4\sigma_u^*$ resonances was confirmed by DFT calculation of the square root of the mean square radius for these orbitals (1.2/1.3/2.0 Å), much lower than that which would result from a Rydberg hydrogen-like behavior.

The occurrence in CO_2 of two well-isolated $K^{-2}V$ peaks, A and B, of different nature, offers a unique opportunity to investigate the evolution of direct and conjugate shake-up processes with photon energy, a question that has been extensively debated in ordinary K^{-1} shake-up. Close to the K^{-2} threshold similar integrated intensities are expected for these two peaks so that their ratio can be predicted close to 2 because the $2\pi^*$ resonance is twofold degenerated. Here at $h\nu = 760$ eV, i.e., ∼100 eV above threshold, the experimental intensity ratio A/B of the conjugate to the direct peak is 1.6, while the theoretical one is about 1.9, both close to 2. The experimental cross sections for the $K^{-2}V$ process $\sigma_{K^{-2}V}$ can be evaluated relatively to the C(K^{-1}) single-hole ionization cross section σ_{SH}, or to the total σ_{1s} cross section [22–24]. The $\sigma_{K^{-2}V}$ cross sections are deduced from the coincident electron counts and from the electron detection efficiencies that decrease regularly from 78 ± 5% at 0 eV to 55 ± 5% at 500 eV. The $\sigma_{K^{-2}V}/\sigma_{1s}$ cross-section ratios are thus estimated to be $(5.2 \pm 1.6) \times 10^{-4}$ for the first peak A; $(3.3 \pm 1.0) \times 10^{-4}$ for the second peak B, and $(1.6 \pm 0.5) \times 10^{-3}$ for the whole $K^{-2}V$ process. The resulting $K^{-2}V$ cross sections are 48 ± 15 b for the first peak A; 30 ± 10 b for the peak B, and 150 ± 45 b for the whole $K^{-2}V$ process. Theoretical (vertical bars) and experimental (open squares) cross sections displayed in Fig. 1 agree within a factor of about 2, which is satisfactory owing to the experimental and theoretical challenges to provide absolute cross sections.

B. Results at $h\nu = 2300$ eV

With a typical resolution $\Delta E/E \approx 2\%$, the magnetic bottle can no longer resolve the conjugate A and direct B peaks 250 eV above threshold. So, in order to study the evolution of the conjugate to direct shake-up satellites on a very broad photon-energy range, we performed experiments on the HAXPES end station of the GALAXIES beamline at the minimum accessible photon energy of 2300 eV, ∼1650 eV above the K^{-2} Double Photo Ionization (DPI) threshold. The electrons are decelerated to a pass energy of 500 eV into the analyzer with 600-μm slits to reach an energy resolution of ∼1 eV. The linear polarization of the photon beam is horizontal and points toward the analyzer. The photoelectron spectrum is shown in Fig. 2. The spectra are strongly dominated by the O(K^{-1}) photoelectron line at 1759.6 eV that could dazzle and saturate the Charge Coupled Device (CCD) detector. To limit such eventual problem the photon flux was reduced by detuning the undulator gap. The O $1s$ ionization threshold in CO_2 is 541.254 eV [25] for $v = 0$ but, since we do not resolve the (∼300 meV) vibrational progression [26], it is safer to take here a centroid value at 541.5 eV that becomes the reference for binding energies of all other states (irrespective from exact analyzer and photon-energy calibration). The peaks at lower kinetic energy (below 1750 eV) correspond to O(K^{-1}) satellites (shake-up). The signal also extends continuously to lower energies, due to core-valence O(K^{-1})V^{-1} double ionization (shake-off), where the carbon $K^{-2}V$ photoelectrons are expected to appear. To make the C($K^{-2}V$) signal visible, a considerably longer acquisition time was necessary to extract the signal from the background statistical fluctuations. Consequently, the signal was accumulated in the 1610–1690 eV kinetic energy range during 15 h with the undulator gap optimized. The signal in the upper red curve in Fig. 2 leads to an improvement of the statistics by a factor of 35. Such statistics is necessary to distinguish by eye, in the inset in Fig. 1, three peaks on a high background. Nevertheless the peak finding and fitting procedure singles them out and gives a good estimate of their positions and areas. The ratio of the C($K^{-2}V$) peaks to the O(K^{-1}) ionization peak is directly deduced from the spectra. The resulting spectrum (with background subtracted) is displayed in Fig. 3 and can be compared with the results at $h\nu = 760$ eV in Fig. 1.

The two experiments give very close binding energies, the values of which are collected in Table I.

The spectra in Figs. 1 and 3 exhibit different heights and widths for the three peaks. The ratio of the relative A/B cross sections appears reversed. However, some cautions must be taken to retrieve the cross sections for A and B because the measured intensities are affected by electron angular distributions in the HAXPES experiment. Since it is not possible to change the photon polarization to vertical nor to rotate the analyzer to the magic angle, we make the restrictive

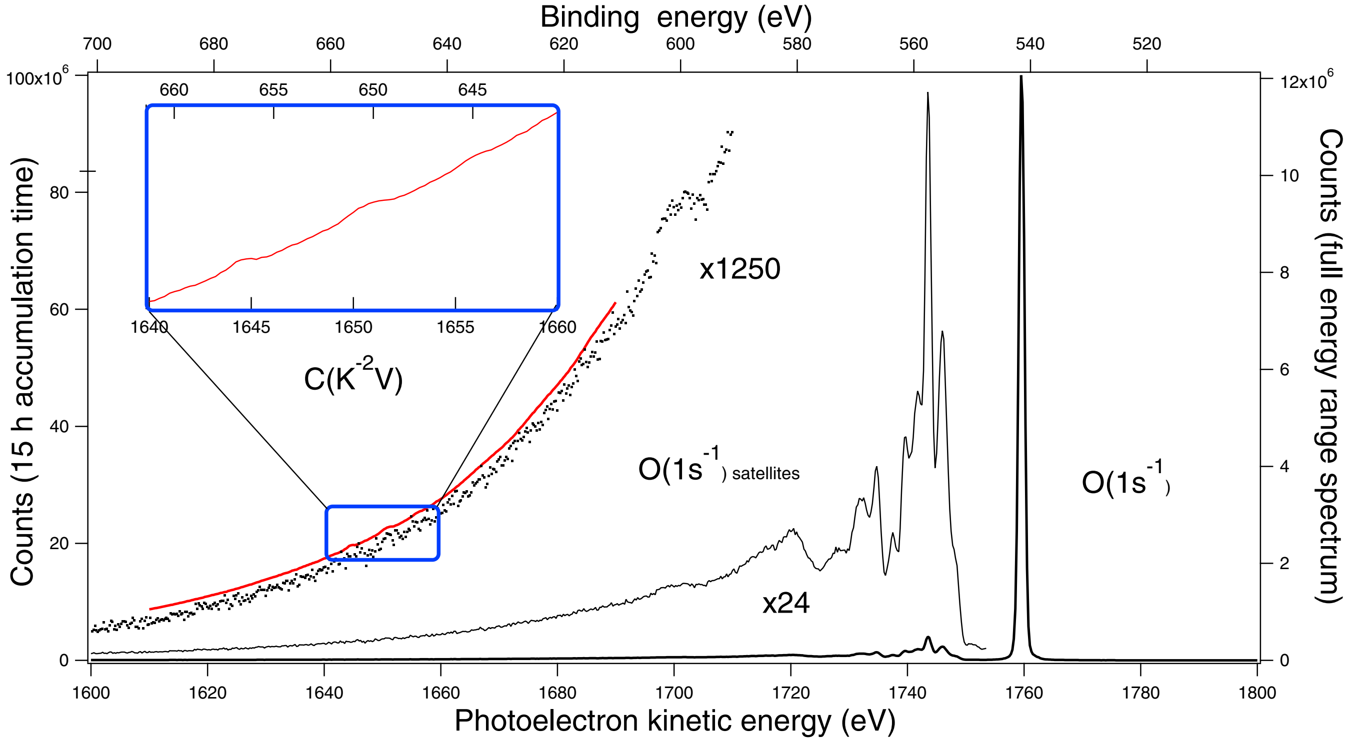

FIG. 2. Photoelectron spectra at $h\nu = 2300$ eV. The spectrum is dominated by the oxygen 1s and satellite lines. By accumulating 1250 times more signal the $C(K^{-2}V)$ lines become visible in the enlarged inset.

assumption that the asymmetry parameter associated to direct shake-up is $\beta = 2$ (p wave) as for the O(1s) photoelectron, and that $\beta = 0$ for the conjugate shake-up (s wave). Considering a half acceptance angle of 20° ± 10° for the entrance lens of the analyzer, a factor 2.8 ± 0.2 appears here between direct ($\beta = 2$) and conjugate shake-up ($\beta = 0$) pathways. This factor

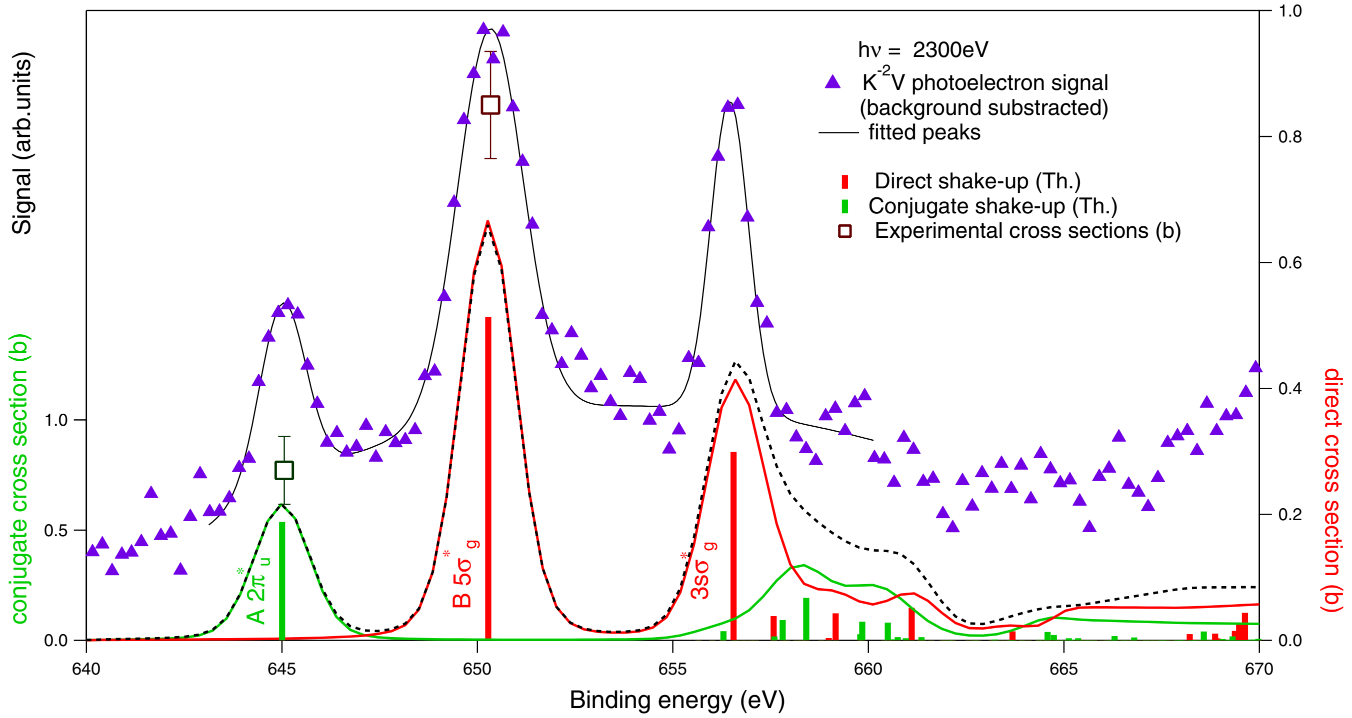

FIG. 3. Comparison of the experimental and theoretical spectra at 2300 eV. The vertical bars correspond to the theoretical cross section and the black squares to the experimental values. To take into account the angular correction factor due to different β parameters for direct ($\beta = 2$) and conjugate ($\beta = 0$) channels the scales differ by a factor of 2.8.

TABLE I. Energy and absolute cross sections at photon energy of 760 and 2300 eV. The binding energies given by the two measurements are in excellent agreement (0.3 eV) within the uncertainties in energy calibration.

Peak	A (conjugate)	B (direct)
BE (eV)	645.6/645.3	650.6/650.5
σ_{Expt}@760 eV	48 ± 15 b	30 ± 10 b
σ_{Expt}@2300 eV	0.76 ± 0.2 b	0.85 ± 0.2 b
σ_{Theor}@760 eV	97 b	50 b
σ_{Theor}@2300 eV	0.5 b	0.5 b

is taken into account to obtain the theoretical spectrum in Fig. 3 and the integrated cross sections for direct and conjugate channels (red and green vertical bars) are displayed on different scaled axes for easier comparison.

Results are summarized in Table I for binding energies (BEs) and cross sections. Given the weakness of the $K^{-2}V$ signal relative to K^{-1}, the agreement between experimental and theoretical cross sections is rather good. The ratio of processes A/B at 760 eV is $1.6 \pm 10\%$; it becomes $0.89 \pm 10\%$ at 2300 eV. The expected decrease of the conjugate channel with respect to the direct channel is observed with increasing photon energy. It is, however, moderate (a factor of 1.8 only) in agreement with our calculations (a factor of 1.9). Apparently, it does not follow the quick decrease observed for valence conjugate shake-up satellites [9]. We believe that our approach provides a better estimate of the evolution of conjugate versus direct channels, as conjugate valence shake-up satellites can be strongly enhanced near threshold by the decay of neutral resonances [27].

In a naive image, one could consider the conjugate channel as excitation of the resonance in the long Lorentzian tail by high-energy photons. The energy conservation is further insured by the shake-off of the other electron in the time allowed by the uncertainty principle. If we consider the Lorentzian tail decrease and a resonance energy $E_0 \sim 300–360$ eV (considering the resonance in the neutral molecule or in the ion), we expect a ratio from 57 to 71 between 760 and 2300 eV, which is close to the experimental ratio $48/0.76 = 63(\pm 30\%)$.

For direct shake-up, the sudden approximation should be valid at high photon energy. In this model, the cross section can be approximated by the C 1s ionization cross section times the overlap (squared) between the C(K^{-1}) frozen core and the final C($K^{-2}V$)B state. This last value is found to be 1.85×10^{-4} in our calculation while the experimental $K^{-2}V/K^{-1}$ value is 3.2×10^{-4}. Such agreement is satisfactory and shows that the excited configuration is properly integrated in the ground state and that the sudden approximation is reasonable.

In the third peak around 656 eV, the direct shake-up contribution $1s \rightarrow 3s\sigma_g$ dominates at $h\nu = 2300$ eV because the conjugate contribution $4\sigma_u^*$ shrinks: a factor 1.8 comes from the energy dependence of the cross section (from A/B ratio) and a factor ∼2.8 from the angular dependence.

Although the ∼1 eV energy resolution of the spectra taken on the GALAXIES beamline is not enough to resolve vibrational progressions in the O(K^{-1}) peak, it is sufficient to see a significant difference between the widths of peaks A and B. The width (1.97 eV) of the $K^{-2}(5\sigma_g^*)$ peak (B) is significantly broader than the experimental resolution and reveals vibrational excitation.

IV. CONCLUSIONS

By using two complementary experimental approaches and a sophisticated theoretical model, we have studied the $K^{-2}V$ excitation process in CO_2.

The advantages of the coincidence technique using the magnetic bottle is to filter out the specific process with the characteristic energy of the C(K^{-2}) Auger electrons. The 4π collection angle provides a signal directly proportional to the different cross sections. The weak point is the degradation in the electron resolution when the photon energy increases. This is circumvented by the HAXPES high-resolution spectra although the C($K^{-2}V$) signal is strongly masked by dominant O(K^{-1}) ionization processes and would have remained invisible without long acquisition time. The good energy resolution can potentially allow a better interpretation of the experimental spectra involving $K^{-2}V$ vibrational excitation.

Our calculations provide a detailed assignment of the C ($K^{-2}V$) spectra and demonstrate the power of such a spectroscopy compared to the $K^{-1}V$ one since the σ_g^* resonances which are dipole forbidden in NEXAFS can be observed here. The CO_2 $K^{-2}V$ spectra are an ideal system as they present two well-isolated direct and conjugate shake-up components. Their absolute cross sections and evolution with photon energy is well reproduced by our calculations. They are believed to provide a better test of the energy dependence of the conjugate versus direct shake-up processes than the usual valence shake-up satellite states.

ACKNOWLEDGMENTS

We are grateful to the PF staff for the stable operation of the storage ring. This work was performed with the approval of the PF Program Advisory Committee (Proposal No. 2010G621). Experiments were performed on the GALAXIES beamline at SOLEIL Synchrotron, France (Proposal No. 20141086). We are grateful to D. Prieur for technical assistance and to the SOLEIL staff for smoothly running the facility.

---

[1] R. Santra, N. V. Kryzhevoi, and L. S. Cederbaum, Phys. Rev. Lett. **103**, 013002 (2009).

[2] P. Lablanquie, F. Penent, J. Palaudoux, L. Andric, P. Selles, S. Carniato, K. Bučar, M. Žitnik, M. Huttula, J. H. D. Eland, E. Shigemasa, K. Soejima, Y. Hikosaka, I. H. Suzuki, M. Nakano, and K. Ito, Phys. Rev. Lett. **106**, 063003 (2011).

[3] M. Nakano, F. Penent, M. Tashiro, T. P. Grozdanov, M. Žitnik, S. Carniato, P. Selles, L. Andric, P. Lablanquie, J. Palaudoux, E.

Shigemasa, H. Iwayama, Y. Hikosaka, K. Soejima, I. H. Suzuki, N. Kouchi, and K. Ito, Phys. Rev. Lett. **110**, 163001 (2013).

[4] J. H. D. Eland, M. Tashiro, P. Linusson, M. Ehara, K. Ueda, and R. Feifel, Phys. Rev. Lett. **105**, 213005 (2010).

[5] M. Nakano, P. Selles, P. Lablanquie, Y. Hikosaka, F. Penent, E. Shigemasa, K. Ito, and S. Carniato, Phys. Rev. Lett. **111**, 123001 (2013).

[6] S. Carniato, P. Selles, L. Andric, J. Palaudoux, F. Penent, M. Žitnik, K. Bučar, M. Nakano, Y. Hikosaka, K. Ito, and P. Lablanquie, J. Chem. Phys. **142**, 014307 (2015).

[7] S. Carniato, P. Selles, L. Andric, J. Palaudoux, F. Penent, M. Žitnik, K. Bučar, M. Nakano, Y. Hikosaka, K. Ito, and P. Lablanquie, J. Chem. Phys. **142**, 014308 (2015).

[8] R. L. Martin and D. A. Shirley, J. Chem. Phys. **64**, 3685 (1976).

[9] B. Kempgens, A. Kivamakï, H. M. Köppe, M. Neeb, A. M. Bradshaw, and J. Fedhaus, J. Chem. Phys. **107**, 4219 (1997).

[10] P. Lablanquie, T. P. Grozdanov, M. Žitnik, S. Carniato, P. Selles, L. Andric, J. Palaudoux, F. Penent, H. Iwayama, E. Shigemasa, Y. Hikosaka, K. Soejima, M. Nakano, I. H. Suzuki, and K. Ito, Phys. Rev. Lett. **107**, 193004 (2011).

[11] K. Ito, F. Penent, Y. Hikosaka, E. Shigemasa, I. H. Suzuki, J. H. D. Eland, and P. Lablanquie, Rev. Sci. Instrum. **80**, 123101 (2009).

[12] G. Goldsztejn, T. Marchenko, R. Püttner, L. Journel, R. Guillemin, S. Carniato, P. Selles, O. Travnikova, D. Céolin, A. F. Lago, R. Feifel, P. Lablanquie, M. N. Piancastelli, F. Penent, and M. Simon (unpublished).

[13] R. Püttner, G. Goldsztejn, D. Céolin, J.-P Rueff, T. Moreno, R. K. Kushawaha, T. Marchenko, R. Guillemin, L. Journel, D. W. Lindle, M. N. Piancastelli, and M. Simon, Phys. Rev. Lett. **114**, 093001 (2015).

[14] J. Rueff, J. M. Ablett, D. Céolin, D. Prieur, T. Moreno, V. Balédent, B. Lassalle-Kaiser, J. E. Rault, M. Simon, and A. Shukla, J. Synchrotron Radiat. **22**, 175 (2015).

[15] D. Céolin, J. M. Ablett, D. Prieur, T. Moreno, J.-P. Rueff, T. Marchenko, L. Journel, R. Guillemin, B. Pilette, T. Marin, and M. Simon, J. Electron Spectrosc. Relat. Phenom. **190**, 188 (2013).

[16] T. X. Carroll, J. Hahne, T. D. Thomas, L. J. Sæthre, N. Berrah, J. Bozek, and E. Kukk, Phys. Rev. A **61**, 042503 (2000), and references therein.

[17] M. Tronc, G. C. King, and F. H. Read, J. Phys. B **12**, 137 (1979).

[18] J.-I. Adachi, N. Kosugi, E. Shigemasa, and A. Yagishita, J. Phys. Chem. **100**, 19783 (1996).

[19] G. R. Wight and C. E. Brion, J. Electron Spectrosc. Relat. Phenom. **3**, 191 (1974).

[20] T. K. Sham, B. X. Yang, J. Kirz, and J. S. Tse, Phys. Rev. A **40**, 652 (1989).

[21] M. N. Piancastelli, J. Electron Spectrosc. Relat. Phenom. **100**, 167 (1999), and references therein.

[22] B. L. Henke, E. M. Gullikson, and J. C. Davis, At. Data Nucl. Data Tables **54**, 181 (1993).

[23] http://henke.lbl.gov/optical_constants/pert_form.html.

[24] M. Schmidbauer, A. L. D. Kilcoyne, H.-M. Köppe, J. Feldhaus, and A. M. Bradshaw, Phys. Rev. A, **52**, 2095 (1995).

[25] K. C. Prince, L. Avaldi, M. Coreno, R. Camilloni, and M. de Simone, J. Phys. B **32**, 2551 (1999).

[26] T. Hatamoto, M. Matsumoto, X.-J. Liu, K. Ueda, M. Hoshino, K. Nakagawa, T. Tanaka, H. Tanaka, M. Ehara, R. Tamaki, and H. Nakatsuji, J. Electron Spectrosc. Relat. Phenom. **155**, 54 (2007).

[27] L. Ungier and T. D. Thomas, Phys. Rev. Lett. **53**, 435 (1984).